Inorganic Chemistry

Article

pubs.acs.org/IC

Structural Stability of Quaternary $ACuFeS_2$ (A = Li, K) Phases: A Computational Approach

Sergio Conejeros,[†] Pere Alemany,[*,†] Miquel Llunell,[†] Víctor Sánchez,[‡] Jaime Llanos,[‡] and Luis Padilla-Campos[§]

[†]Departament de Quimica Física and Institut de Química Teòrica i Computacional (IQTCUB), Universitat de Barcelona, Diagonal 647, 08028 Barcelona, Spain

[‡]Departamento de Química, Facultad de Ciencias, Universidad de Católica del Norte, Casilla 1280, Antofagasta, Chile

[§]Departamento de Química, Facultad de Ciencias Básicas, Universidad de Antofagasta, Casilla 170, Antofagasta, Chile

ABSTRACT: At ambient conditions, the quaternary sulfides $LiCuFeS_2$ and $KCuFeS_2$ present totally different crystal structures: while $LiCuFeS_2$ crystallizes in a trigonal $CaAl_2Si_2$-type structure, a tetragonal $ThCr_2Si_2$-like structure is found for $KCuFeS_2$. In this work, we present a computational study describing first the changes in the structural preference of the $ACuFe_2$ phases as a function of the alkali ion and second, the structural stability of the $CuFeS_2$ phases obtained by electrochemical removal of the alkali cations from the two $ACuFeS_2$ compounds. A high copper mobility is found to be responsible for the observed metastability of the layered trigonal $CuFeS_2$ phase obtained by delithiation of $LiCuFeS_2$. In contrast, the tetragonal $CuFeS_2$ structure obtained removing potassium from $KCuFeS_2$ is predicted to be stable, both from the kinetic and thermodynamic points of view. The possibility of stabilizing mixed $Li_xCu_{1-x}FeS_2$ phases with a $ThCr_2Si_2$-type structure and the mobility of lithium in these is also explored.

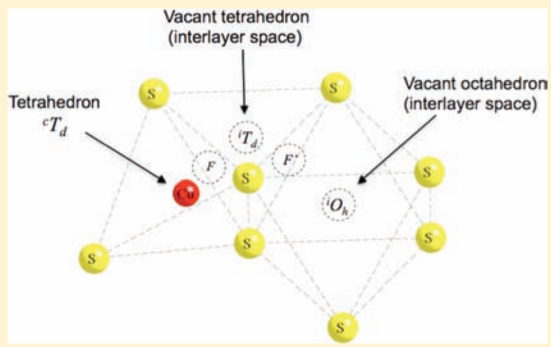

■ INTRODUCTION

Alkali metals react with chalcopyrite to form quaternary phases with $ACuFeS_2$ (A = alkali metal) stoichiometry.[1−6] Depending on the size of the alkaline ions, these intercalated compounds crystallize either in a trigonal $CaAl_2Si_2$-type (for A = Li, Na) or a tetragonal $ThCr_2Si_2$-type (for A = K, Rb, Cs) structure (Figure 1). Structural and electronic properties were studied for these compounds from both the theoretical and experimental points of view.[7−10] In the two alternative structures, the $ACuFeS_2$ phases present a layered structure with the alkaline atoms occupying sites between successive $CuFeS_2$ layers formed by condensation of edge sharing MS_4 tetrahedra with a random distribution of Cu and Fe atoms at their centers. An analysis of the electronic structure for these compounds revealed that, as expected, the nature of the alkaline atoms in the structure is mainly ionic while the bonds in the $CuFeS_2$ layers have a significant covalent component.[11]

From the experimental point of view, for the specific case of $LiCuFeS_2$, the removal of lithium atoms yields a metastable 2D trigonal $CuFeS_2$ phase that reorganizes upon heating up to 613 K to the original 3D tetragonal chalcopyrite structure.[1] This phase transition prevents the use of this compound as a cathode for secondary batteries. Contrary to what is observed for $LiCuFeS_2$, it has been shown experimentally that it is possible to remove completely all potassium from $KCuFeS_2$ with the $ThCr_2Si_2$-type structure to yield a stable tetragonal 2D $CuFeS_2$ phase in which even large organic cations may be intercalated.[12]

Despite the experimental and theoretical work devoted to these compounds, some open questions about their physical and chemical properties remain still open, offering an excellent opportunity to show the ability of modern density functional theory based methods to explain the origin of experimental observations at an atomic level. In this case it is of interest to clarify first the details on the different structural choice found for $LiCuFeS_2$ and $KCuFeS_2$. The second question to be answered is the origin of the different stabilities of the layered $CuFeS_2$ phases obtained after removing the alkali atoms. The phase transition that has been observed for the trigonal $CuFeS_2$ layered structure obtained from $LiCuFeS_2$ has been attributed to the diffusion of copper atoms toward the interlayer space in the absence of lithium, although, to the best of our knowledge, no clear confirmation of this hypothesis has been presented. However, it is not obvious why the diffusion of copper is not favored when the material contains lithium or why copper diffusion is hindered in the tetragonal $CuFeS_2$ phase obtained from $KCuFeS_2$. The answer to these questions must consider the different activation energies for copper (and iron) diffusion in the two alternative 2D phases. This system provides, in our opinion, a nice example of the strong relation between the observed stability of a compound and the mobility of ions within its crystal structure, a question that can be properly

Received: August 12, 2011
Published: December 16, 2011

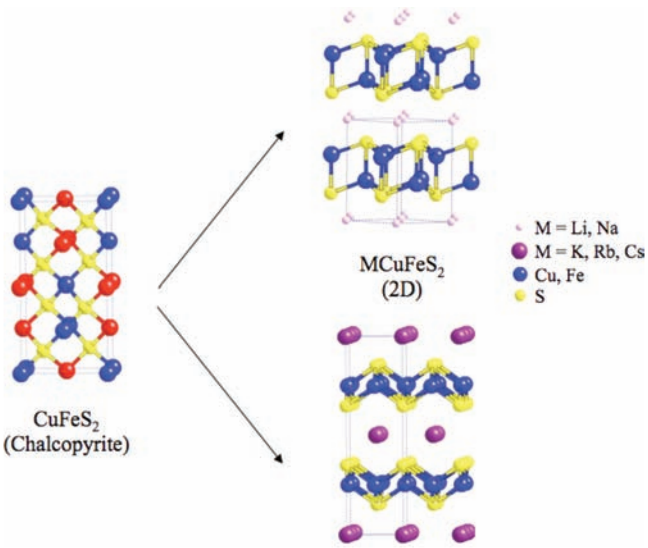

Figure 1. Chalcopyrite (left) reacts with alkali metals to give two alternative layered structures, the trigonal $CaAl_2Si_2$-type (upper right) and the tetragonal $ThCr_2Si_2$-type (lower right) structures, depending on the size of the alkali metal atoms.

addressed with total energy calculations using accurate first-principles quantum chemical methods.

The aim of the present work is to address, using first-principles, density functional theory based methods, first the relative stability of the $CaAl_2Si_2$ and $ThCr_2Si_2$-type phases for $ACuFeS_2$ compounds when A = Li or K, and second to study in detail the copper diffusion in the related 2D structures for $CuFeS_2$. A possible transition path is proposed and an estimation of the activation energy involved in the process is calculated. The last question that is addressed is the possibility of stabilizing lithium containing $Li_xK_{1-x}CuFeS_2$ phases with a tetragonal $ThCr_2Si_2$ structure that combines in a same compound high mobility Li ions while preventing the breakdown of the layered host $CuFeS_2$ structure when lithium atoms leave their original positions. These calculations allow us also to obtain estimates for the diffusion coefficients for copper, iron and alkali metal ions in the two structures as well as the average intercalation voltage for hypothetical $LiCuFeS_2$ with a tetragonal $ThCr_2Si_2$-type structure.

■ METHODOLOGY AND COMPUTATIONAL DETAILS

First-principles electronic structure calculations for several Li_xCuFeS_2, K_xCuFeS_2, and $Li_xK_{1-x}CuFeS_2$ models with a varying quantity of alkaline metal ions have been carried out using a numerical, atomic orbitals DFT-based approach which has been developed for efficient calculations in large systems and implemented in the SIESTA code.[13−15] Exchange and correlation effects were described using the generalized gradient approximation (GGA) to DFT and, in particular, the PBE[16] functional. $ACuFeS_2$ and their derived $CuFeS_2$ phases present a complex electronic structure due to the presence of unpaired electrons on the Fe^{2+}/Fe^{3+} cations. To tackle with this problems, spin polarized calculations have been employed in order to take into account the effect of the presence of iron cations with unpaired electrons on the structural preferences for these phases.

Only the valence electrons are considered in the calculations, with the atomic cores being replaced by norm-conserving Troullier−Martins pseudopotentials[17] factorized in the Kleinman−Bylander form.[18] Valence electrons were treated explicitly using an atomic orbital basis set of triple-ζ plus polarization (TZP) quality for copper and iron, and of double-ζ plus polarization (DZP) quality for sulfur, lithium, and potassium atoms, all of them obtained with an energy shift of 100 meV.[19] The energy cutoff of the real space integration mesh was set to 150 Ry and the Brillouin zone was sampled using grids of ($8 \times 8 \times 8$) k-points[20] in all calculations using single cells.

Supercells of both structural types with 18 formula units each were used to explore the relative stability of $Li_xK_{1-x}CuFeS_2$ phases with different Li to K ratios. The same approach was used to calculate the activation barriers for Li and K diffusion in $ACuFeS_2$ (A = Li or K) with a $ThCr_2Si_2$-type structure introducing a single alkali metal vacancy in the supercell. In this case it has been verified that these models are large enough to prevent the periodic images of the defect to have a significant interaction.

■ RESULTS AND DISCUSSION

Structural Choice for the $ACuFeS_2$ phases. As mentioned in the introduction, $LiCuFeS_2$ and $KCuFeS_2$ crystallize in two different structures (Figure 1). The crystal structure for $LiCuFeS_2$ is a trigonal, $CaAl_2Si_2$-type structure. Tetracoordinated copper and iron atoms occupy vertex sharing tetrahedral sites in the covalent layers with a random distribution, while lithium atoms occupy a fairly distorted octahedral hole formed by six sulfur atoms from two successive $CuFeS_2$ covalent layers, three of them on each layer. In the space between covalent layers we find also an equal number of empty distorted tetrahedral sites, each of them surrounded by three edge-sharing octahedral sites occupied by lithium cations. The experimentally determined unit cell dimensions as well as the principal structural parameters for $LiCuFeS_2$ can be found in Table 1.

Table 1. Unit Cell Dimensions and Principal Structural Parameters for the Experimentally Determined Crystal Structures of $LiCuFeS_2$ [1] and $KCuFeS_2$ [3]

	Li $CuFeS_2$	$KCuFeS_2$
structure type	$CaAl_2Si_2$ ($P\bar{3}m1$, No. 164)	$ThCr_2Si_2$ ($I4/mmm$, No. 139)
cell parameters (Å)	a = 3.807; c = 6.352	a = 3.837; c = 13.384
cell volume (Å^3)	79.73	197.047
M−S distances (Å)	2.342, 2.419	2.345
M−M distance (Å)	2.725	2.713
A−S distance (Å)	2.697	3.369

On the other hand, $KCuFeS_2$ crystallizes in a tetragonal $ThCr_2Si_2$-type structure that is also formed by successive $CuFeS_2$ covalent layers separated by potassium cations. Copper and iron occupy the centers of MS_4 tetrahedra in a random distribution. Tetrahedra in this case share edges to form $CuFeS_2$ layers with sulfur atoms arranged in square nets. As a consequence, potassium cations have each eight sulfur atoms as neighbors in a distorted cubic coordination sphere, with two squares of sulfur atoms belonging to two successive $CuFeS_2$ layers. The experimentally determined unit cell dimensions as well as the principal structural parameters for $KCuFeS_2$ are shown in Table 1.

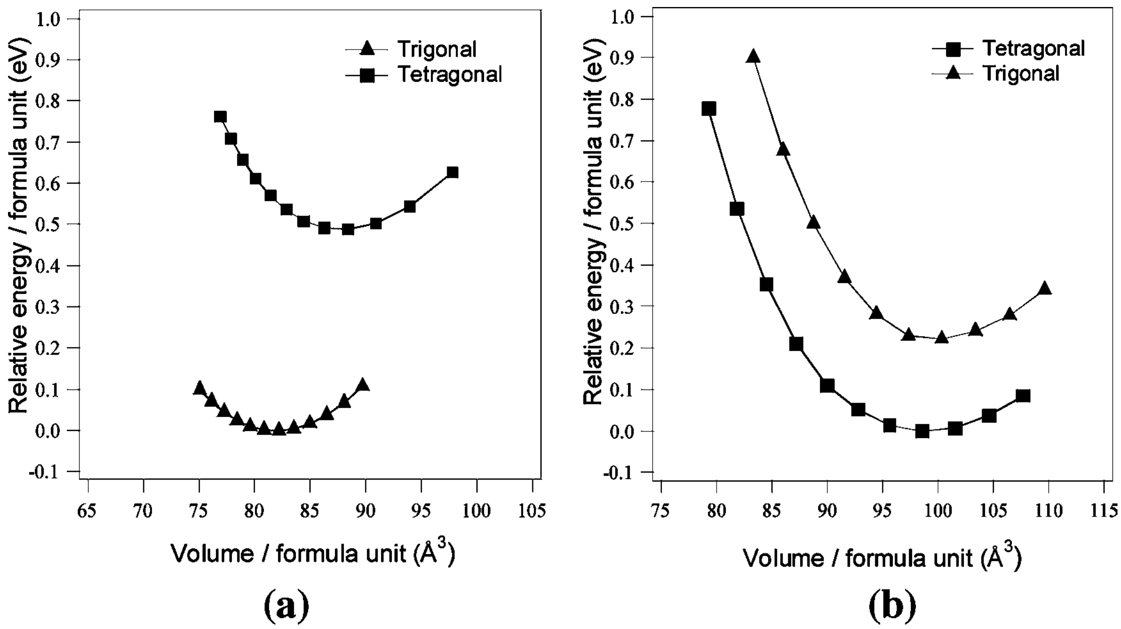

Figure 2. Energy versus volume curves for (a) the stable trigonal (triangles) and the hypothetical tetragonal $LiCuFeS_2$ phases (squares) and (b) for the stable tetragonal (squares) and hypothetical trigonal $KCuFeS_2$ phases (triangles).

We have calculated the energy versus volume curves for $LiCuFeS_2$ and $KCuFeS_2$ in the two alternative structures. To tackle with the disorder of the occupation of the MS_4 tetrahedra by either Cu or Fe atoms we have used the simplest models for the two structures in which the transition metal atoms occupy the tetrahedral sites within each covalent layer in a completely ordered arrangement compatible with the smallest unit cell, that is with $Z = 1$ and $Z = 2$ formula units for the $CaAl_2Si_2$ and the $ThCr_2Si_2$-type structures, respectively. Since the actual distribution of Fe and Cu atoms cannot be determined unambiguously from the experimental data, we have not attempted to determine if there is any significant coupling between the spins on neighboring iron atoms, and consider, as an approximation, only the ferromagnetic solution with all unpaired spins on iron atoms aligned in the same direction.

The energy versus volume curves calculated for $LiCuFeS_2$ (Figure 2a) show that the experimentally observed $CaAl_2Si_2$-type structure is indeed more stable than the $ThCr_2Si_2$-type one. The equilibrium volume and the bulk modulus for the two alternative structures (Table 2) have been obtained from a fit of the energy versus volume curves to the Murnaghan equation.[21]

Table 2. Unit Cell Dimensions, Bulk Modulus, and Principal Structural Parameters Calculated for the Equilibrium $CaAl_2Si_2$ and $ThCr_2Si_2$-Type Structures for $LiCuFeS_2$[a]

structure	$CaAl_2Si_2$-type	$ThCr_2Si_2$-type
a (Å)	3.848 (+1.1%)	3.748
c (Å)	6.405 (+0.8%)	12.495
V_0 (Å^3)	82.14 (+3.0%)	175.49
B (GPa)	50.0	48.5
M−S (Å)	2.371 (+1.2%)	2.401
	2.427 (+0.3%)	
M−M (Å)	2.734 (+0.3%)	2.664
Li−S (Å)	2.723 (+1.0%)	3.109

[a]Deviations with respect to the experimentally determined structure (see Table 1) are indicated in parentheses.

The cell parameters obtained for the optimized structure (Table 2) are in good agreement with the experimental ones, although a direct comparison is not straightforward since we have assumed an ordered arrangement of Cu and Fe atoms. If we compare with some earlier calculations[22] where spin polarization was not considered, when spin polarization is allowed, the occupation of formally antibonding Fe−S orbitals leads to a significant enlargement of the metal centered tetrahedra that results in a larger volume per unit cell and a much better agreement with the available experimental data.

The energy difference between the two alternative structures for $LiCuFeS_2$ is not excessively large, 0.49 eV per formula unit, but since the observed $CaAl_2Si_2$-type structure has a smaller volume per formula unit than the hypothetical $ThCr_2Si_2$-type one, it is not possible to increase the pressure to stabilize $LiCuFeS_2$ with such a structure.

In Figure 2b, we show the energy versus volume curves calculated for $KCuFeS_2$ in the two alternative structures. As in the previous case, calculations agree with the experimental observation and indicate that in this case the most stable structure corresponds to the tetragonal $ThCr_2Si_2$-type. Structural information for the two optimized structures of $KCuFeS_2$ is given in Table 3.

In this case the energy difference, 0.22 eV, between the two alternative structures is even smaller than for $LiCuFeS_2$. Since the hypothetical $CaAl_2Si_2$-type structure has a smaller volume per formula unit than the most stable $ThCr_2Si_2$-type one, it should, in principle, be possible to stabilize $KCuFeS_2$ in the $CaAl_2Si_2$-type applying some pressure. An estimation of the pressure needed at $T = 0$ K can be obtained by equating the entalphy of the two phases. Following this procedure we predict that a pressure of approximately 71 GPa should be applied to $KCuFeS_2$ to obtain it in a $CaAl_2Si_2$-type structure.

Considering these results it is interesting to ask if it could be possible to stabilize a tetragonal $ThCr_2Si_2$-type phase by replacing some of the lithium ions in $LiCuFeS_2$ by potassium. To answer it we have compared the energies of supercells containing 18 formula units with the two alternative structures

Table 3. Unit Cell Dimensions, Bulk Modulus, and Principal Structural Parameters Calculated for the Equilibrium $CaAl_2Si_2$, and $ThCr_2Si_2$-Type Structures for $KCuFeS_2$[a]

structure	$CaAl_2Si_2$-type	$ThCr_2Si_2$-type
a (Å)	3.993	3.851 (+0.4%)
c (Å)	7.261	13.308 (−0.6%)
V_0 (Å^3)	100.28	197.46 (+0.2%)
B (GPa)	52.4	38.3
M−S (Å)	2.378	2.413 (+2.9%)
	2.425	
M−M (Å)	2.821	2.724 (+0.4%)
K−S (Å)	3.095	3.306 (−1.9%)

[a]The errors with respect to the experimentally determined structure (see Table 1) are indicated in parentheses.

for $Li_xK_{1-x}CuFeS_2$ solid solutions with different Li/K ratios. In all cases we have considered only models with the same Li/K ratio for all layers in the supercell, avoiding structures with different cationic layers. According to our calculations (Figure

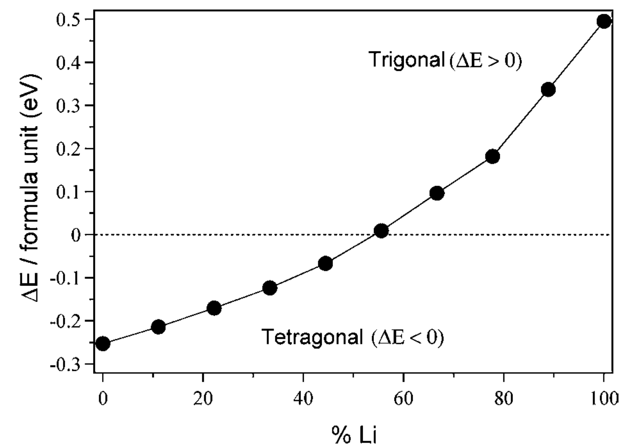

Figure 3. Energy difference between the $ThCr_2Si_2$ and the $CaAl_2Si_2$-type structures as a function of the percentage of lithium for $Li_xK_{1-x}CuFeS_2$ solid solutions. Negative values for ΔE indicate that the $ThCr_2Si_2$-type structure is more stable.

3), the maximal quantity of lithium that may be inserted in a Li/K mixed phase with a tetragonal $ThCr_2Si_2$-type structure lies around 55%, percentage for which the two alternative structures have practically the same energy per formula unit.

Copper Mobility in the Layered $CuFeS_2$ Phases. When lithium atoms are removed completely from $LiCuFeS_2$ the resulting layered trigonal $CuFeS_2$ structure is not stable and a phase transition to tetragonal chalcopyrite is observed upon application of moderate temperatures. The origin of this behavior has been attributed to a high mobility of copper atoms in the trigonal layered $CuFeS_2$ structure,[1] a situation that is not observed for the stable 2D tetragonal structure obtained upon removal of potassium from $KCuFeS_2$.[12]

The analysis of the behavior of copper ions in the bidimensional $CuFeS_2$ structures requires in a first approximation the establishment of probable diffusion paths for the movement of copper (and possibly of iron) atoms from the covalent layers into the interlayer region. For this purpose, we have realized a series of calculations in which the copper (or iron) atoms occupy different positions in the two layered $CuFeS_2$ frameworks.

Let us first consider the structure resulting from complete lithium removal from the $CaAl_2Si_2$-type structure of $LiCuFeS_2$. As shown in Figure 4a, the copper atoms initially located in the

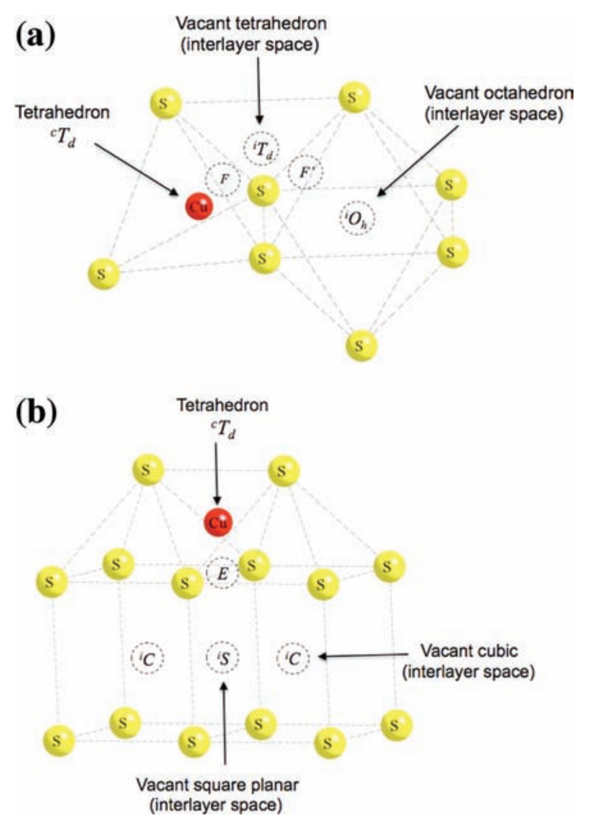

Figure 4. Crystal structure showing the sites relevant for copper migration in the $CuFeS_2$ phases obtained by complete removal of the alkali metal ions from (a) $LiCuFeS_2$ and (b) $KCuFeS_2$.

covalent layers may leave their original tetrahedral ^cT_d sites passing through one of the triangular faces (F) to end in an interlayer tetrahedral site ^iT_d. Once in the interlayer region the metal atoms may further proceed via another triangular face (F′) to one of the neighboring empty octahedral sites ^iO_h that are fully occupied by lithium cations in the parent $LiCuFeS_2$ phase. Note that a new 3D crystal structure with segregated Cu and Fe layers is reached if all copper atoms move from the ^cT_d sites to the ^iT_d ones. This 3D structure does, however, not coincide with that of chalcopyrite and a further rearrangement is needed to reach the experimentally observed chalcopyrite structure. Since the aim of this work is to understand the different stability for the $CuFeS_2$ structures obtained upon removal of the alkali metal atoms from the two different $ACuFeS_2$ compounds, we will limit our investigation to the diffusion of transition metals into the interlayer region to give the intermediate 3D $CuFeS_2$ structures with alternating Cu and Fe layers, assuming that this initial diffusion process is the rate determining step in the experimentally observed transformation.

To estimate the activation energy for transition metal diffusion in the trigonal $CuFeS_2$ structure we have evaluated the energy profile locating the metal atoms at the relevant points (^cT_d−F−^iT_d−F′−^iO_h) of this path. As discussed above, the effect of spin polarization is to yield larger unit cells, and hence larger S_3 triangles through which the copper ions must pass to reach the interlaminar space. For this reason it is

dx.doi.org/10.1021/ic201758j | Inorg. Chem. 2012, 51, 362−369

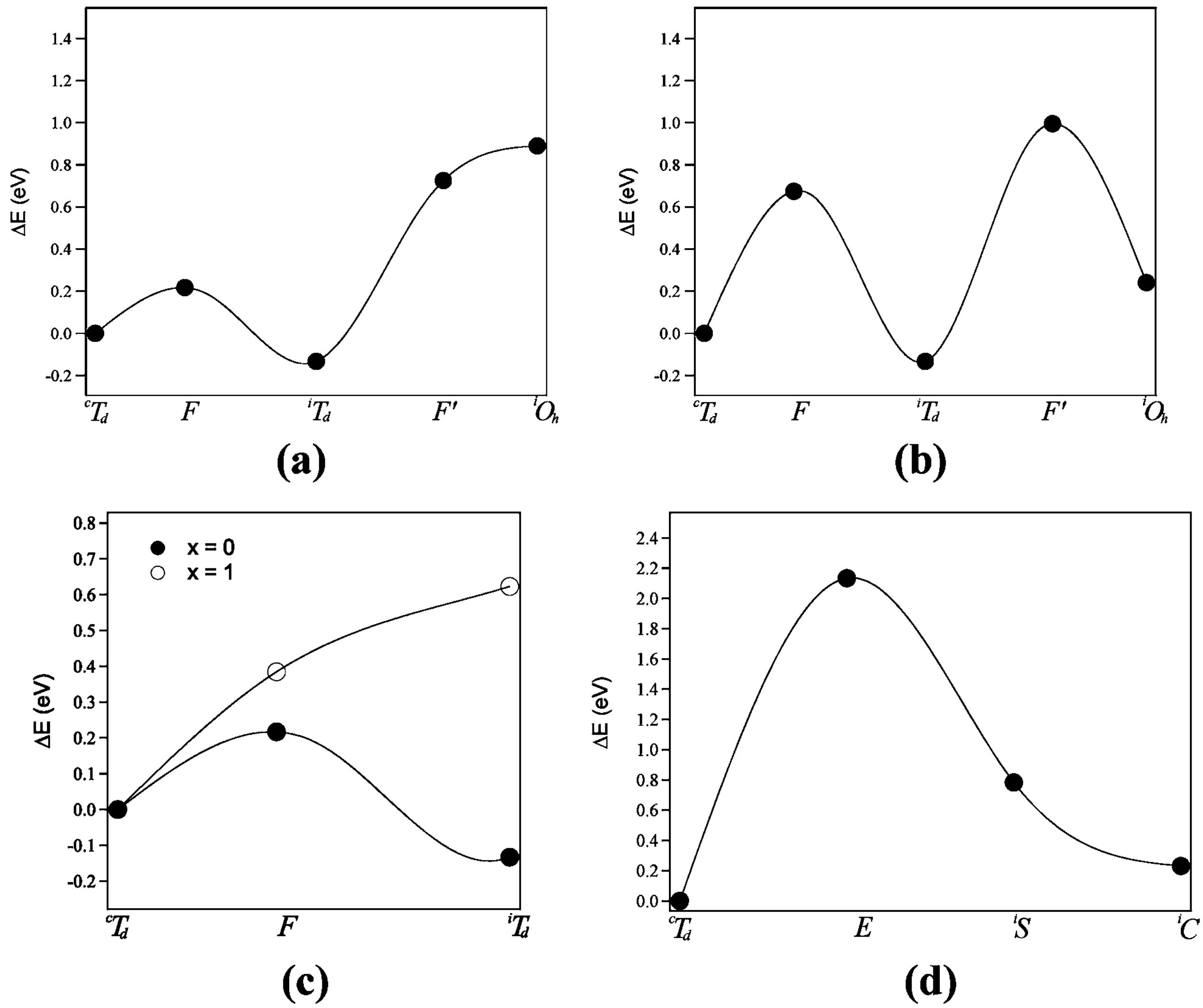

Figure 5. Energy profiles for transition metal migration in the $ACuFeS_2$ phases. (a) Copper migration in trigonal $CuFeS_2$, (b) Iron migration in trigonal $CuFeS_2$, (c) comparison between copper migration in trigonal Li_xCuFeS_2, and (d) Copper migration in tetragonal $CuFeS_2$.

imprescindible to consider the possibility of spin polarization in the calculation in order to obtain a good approximation of the activation energy for copper diffusion in these compounds. Since copper and iron occupy exactly the same sites in the crystal structure we have also analyzed the possibility of iron diffusion following the same ${}^{c}T_d$–F–${}^{i}T_d$–F′–${}^{i}O_h$ path.

It is not possible to optimize the geometry for the initial $CuFeS_2$ structure since copper atoms move spontaneously from the ${}^{c}T_d$ to the ${}^{i}T_d$ sites during the optimization process, and we have taken the geometry of the initial $CuFeS_2$ structure from a complete optimization of the parent $LiCuFeS_2$ phase (see Table 1). This structure is used to obtain the energies for the cases with copper either in their original ${}^{c}T_d$ sites or at the F position. For the structures with copper atoms either in the intralayer ${}^{i}T_d$ or at the F′ position we have used the intermediate structure with segregated copper and iron layers obtained from a complete optimization of the trigonal $CuFeS_2$ structure, and for the calculations with copper in the ${}^{i}O_h$ sites we use the structure obtained from an optimization with the copper in these sites. Since iron and copper occupy identical positions in the parent structure, the same structures may be used to analyze the migration of iron atoms.

Before analyzing the energetics of the diffusional path in the trigonal structure let us analyze the situation for the alternative tetragonal $CuFeS_2$ phase obtained by removal of the potassium atoms from the $ThCr_2Si_2$-type structure for $KCuFeS_2$. Although the crystal structure is quite different to that found for $LiCuFeS_2$, we still think it is pertinent to ask for the possibility of copper diffusion in this structure. In order to analyze this possibility we have considered the migration path shown in Figure 4b. In the $ThCr_2Si_2$-type structure, copper and iron occupy each tetrahedral sites in the covalent layer. Following the convention used above for the trigonal case we will label these sites as ${}^{c}T_d$. In the $ThCr_2Si_2$-type structure four of these tetrahedra share their vertices in such a way that they surround an empty square pyramidal site. The interlayer region in this structure is quite simple and the potassium atoms in $KCuFeS_2$ sit in the center of distorted cubic coordination sites forming a square array. When potassium is removed from $KCuFeS_2$ we get a structure with empty cubic sites (${}^{i}C$) in the interlayer region. Two alternative pathways for the migration of copper or iron from the initial ${}^{c}T_d$ sites to the ${}^{i}C$ ones can be envisaged from the figure. In the first, the metal atom moves directly from the covalent layer to the interlayer region passing through one of the edges of the tetrahedron (E position) to proceed further

Table 4. Calculated Activation Energies and Diffusion Constants for Copper and Iron in the Trigonal $CuFeS_2$ Structure at 300 and 613 K

atom	diffusional path $i \to j$	E_a (eV)	D_{ij}^0 (cm^2/s)	$D_{i\to j}$ (300 K) (cm^2/s)	$D_{i\to j}$ (613 K) (cm^2/s)
copper	${}^cT_d \to {}^iT_d$	0.22	3.47×10^{-2}	7.00×10^{-6}	5.40×10^{-4}
iron	${}^cT_d \to {}^iT_d$	0.67	6.56×10^{-3}	3.64×10^{-14}	2.03×10^{-8}

to a square planar coordination site (${}^iS$) in the interlayer zone and finally to reach the cubic site ${}^iC$. A detailed geometrical analysis of the second path proceeding through the empty square pyramids allows us to discard this possibility because of the unreasonably short M−S distances implied.

Figure 5 shows the energy profiles for copper (Figure 5a) and iron (Figure 5b) diffusion in the trigonal $CuFeS_2$ structure. In all cases, the most stable structure corresponds to that with the diffusing atoms in the tetrahedral holes of the interlayer region. The low activation energy found for copper, 0.22 eV, for the movement through the triangular face F is in good agreement with the suggestion deduced from experimental observations that the transition from the 2D trigonal structure of $CuFeS_2$ to a tetragonal one starts with the diffusion of copper atoms into the intrerlayer region. It is also consistent with the fact that when we attempted an optimization of the initial trigonal $CuFeS_2$ structure with all metal atoms in ${}^cT_d$ sites, a displacement of the copper atoms takes place to end in the intermediate structure with copper atoms in the ${}^iT_d$ sites and iron atoms in the ${}^cT_d$ ones. In contrast to what is observed for copper, the barrier calculated for iron migration on the same path is much higher, 0.67 eV, allowing us to state that only copper diffusion should be relevant at the temperature at which the phase transition is observed. For the movement of copper atoms from the ${}^iT_d$ to the ${}^iO_h$ site, we find a much higher activation energy suggesting that this process should not be relevant in the posterior changes to reach the final chalcopyrite structure.

In Figure 5c, we show the energy profile calculated for the trigonal Li_xCuFeS_2 structure for the limiting cases with $x = 0$ and $x = 1$. As already discussed, complete removal of lithium leads to a low activation energy for copper hopping from the initial ${}^cT_d$ to the ${}^iT_d$ site through the triangular F site. The presence of lithium atoms in the ${}^iO_h$ sites as in the original $LiCuFeS_2$ structure prevents the movement of copper from the ${}^cT_d$ to the ${}^iT_d$ sites, a situation that can be explained by the strong electrostatic interactions when all sites in the interlayer region, both tetrahedral and octahedral, are occupied by charged species. An intermediate behavior between the two limiting situations shown in Figure 5c is expected for an intermediate lithium contents.

The energy profiles for copper migration in the $ThCr_2Si_2$-type structure obtained by potassium removal from $KCuFeS_2$ are shown in Figure 5d. A considerable activation energy is predicted, 2.1 eV, in good agreement with experimental observations: in contrast to what is found for trigonal $CuFeS_2$, the tetragonal structure is predicted to be stable, both from the thermodynamic and kinetic points of view.

With the purpose of relating the migration probability of copper with temperature, a classical transition state model to estimate the diffusion constants has been used. For a copper atom hopping from an i to a j site, we can write[23]

$$D_{i\to j} = D_{ij}^0 e^{-E_a/kT} \tag{1}$$

with

$$D_{ij}^0 = \frac{n\nu_i l^2}{2d} \tag{2}$$

where E_a is the activation energy associated with the $i \to j$ jump, ν_i is the frequency at the equilibrium geometry for the "i" site, l is the minimum distance between two adjacent sites (in this case between the ${}^cT_d$ and ${}^iT_d$ sites), d is the dimensionality of the diffusional space, and n number of ways in which copper atoms can migrate from ${}^cT_d$ to the ${}^iT_d$ sites.[24]

To determine the frequency ν_i, we assume that the hopping atom is trapped in the ${}^cT_d$ sites by a harmonic potential. Therefore ν_i can be calculated through the expression

$$\nu_i = \frac{1}{2\pi}\sqrt{\frac{k_i}{M}} \tag{3}$$

where M is the mass of the hopping atom and k_i the force constant that within the harmonic approximation can be defined as[25]

$$k_i \approx \frac{2[E_i(r_{\min} + \Delta r) - E_i(r_{\min})]}{[(r_{\min} + \Delta r) - r_{\min}]^2} \tag{4}$$

where $r_{\min}$ and Δr represent the minimum energy position (the ${}^cT_d$ site) and the displacement of the atom along the diffusional path, respectively.

In Table 4, we show the activation energies and diffusion constants for copper at 300 and 613 K. According to our calculations the probability of copper diffusion from the ${}^cT_d$ sites toward the ${}^iT_d$ holes increases with the temperature raise about 2 orders of magnitude. Thus, it is reasonable to suggest that at 613 K the increased diffusion of copper could be at the origin for the observed phase transition from a layered to a chalcopyrite structure, that is, to a 3D solid. Calculation of the diffusion constant for iron shows that it is completely irrelevant at the temperatures for which the transition has been observed.

Diffusion of Lithium and Potassium in the $ThCr_2Si_2$-Structure. As discussed above, our calculations suggest the possibility of stabilizing mixed $Li_xK_{1-x}CuFeS_2$ solid solutions with a $ThCr_2Si_2$-structure and a lithium content of up to $x = 0.55$. In principle, these hypothetical phases would combine the structural stability conferred by the potassium cations with the presence of fast diffusing lithium ions. To explore the cationic mobility in such structures, we have calculated the diffusion constants for Li and K in the $ThCr_2Si_2$-type structure using a supercell model with a single vacancy for the two limiting $LiCuFeS_2$ and $KCuFeS_2$ stoichiometries using the optimized structures for each case.

The calculated harmonic frequencies v_i (eq 1) for the alkali ions trapped in the ${}^iC$ sites of the $ThCr_2Si_2$-type structure are about 10^{13} Hz, lying in the range of phonon frequencies and consistent with typical estimations for this magnitude in other compounds.[26] The diffusion coefficient for lithium in a $ThCr_2Si_2$-type structure at room temperature is about 10^{-8} $cm^2 s^{-1}$, about 17 orders of magnitude larger than the one

dx.doi.org/10.1021/ic201758j | Inorg. Chem. 2012, 51, 362−369

Table 5. Calculated Activation Energies and Diffusion Constants for Lithium and Potassium in the Tetragonal $CuFeS_2$ Structure at 300 K

atom	diffusional path $i \to j$	E_a (eV)	D_{ij}^0 (cm^2/s)	$D_{i\to j}$ (300 K) (cm^2/s)
lithium	$^iC \to {}^iC$	0.26	6.24×10^{-3}	2.52×10^{-7}
potassium	$^iC \to {}^iC$	1.34	4.37×10^{-3}	1.54×10^{-25}

calculated for potassium. These results suggest that in a hypothetical mixed $Li_xK_{1-x}CuFeS_2$ phase, the potassium cations would remain in their original positions, preventing in this way the collapse of the framework, while the lithium ions would be free to diffuse in the interlaminar regions. Considering that for commercially used materials such as Li_xCoO_2 the diffusion coefficient has been found to be within the range of 10^{-13} to 10^{-7} cm^{2}s^{-1} at room temperature,[27] mixed $Li_xK_{1-x}CuFeS_2$ phases could be envisaged as acceptably fast Li diffusion materials.

Average Lithium Insertion Voltage. The open-cell voltage that could be obtained from lithium intercalation between a lithium anode and a cathode built from a mixed $Li_xK_{1-x}CuFeS_2$ phase depends on the lithium chemical potential in the cathode. Although it is not possible to calculate the open-cell voltage as a continuous function of the amount x of lithium in the cathode material using only total-energy methods, it has been suggested[28] that a useful estimation for this parameter can be obtained from the average intercalation voltage determined for the limiting stoichiometry with $x = 1$. In this case one lithium ion per formula unit can be removed from $LiCuFeS_2$ and the insertion reaction is written as

$$CuFeS_2 + Li \to LiCuFeS_2$$

The average intercalation voltage, $\overline{V}$, can be obtained from the Gibbs free energy difference for this process that can be estimated[29−33] from the total energies of the three compounds if entropy and volumetric effects are ignored:

$$\overline{V} = \frac{E[CuFeS_2] + E[Li] - E[LiCuFeS_2]}{F}$$

where E refers to the total energy per formula unit of each compound, the optimized *bcc* structure of lithium has been considered, and F is the Faraday constant.

Following this procedure we obtain an average intercalation voltage of 1.8 V, considerably lower than the 3.75 V calculated for $LiCoO_2$, but in the range found for the hypothetical $LiCoS_2$ (2.05 V) or $LiCoSe_2$ (1.46 V) compounds.[33] Our calculated voltage is in good agreement with the observation that, in general, sulfides have lower intercalation voltages than oxides[28,34] and are, hence, poor candidates for efficient cathode materials in Li^+ batteries.

CONCLUSIONS

We have used state-of-the-art first-principles total energy methods based on density functional theory to study the $ACuFeS_2$ phases with A = Li or K. Our calculations confirm the experimental observation that for small cations such as lithium a trigonal $CaAl_2Si_2$-type structure is favored over the alternative tetragonal $ThCr_2Si_2$-type structure, while for larger cations such as potassium the opposite situation is found. Our study reveals that, in principle, a mixed $Li_xK_{1-x}CuFeS_2$ phase with a $ThCr_2Si_2$-type structure and a lithium contents up to x = 0.55 could be synthesized.

We have also addressed the stability of the $CuFeS_2$ phases obtained by cation removal of the parent $ACuFeS_2$ phases. While fast copper ion diffusion is predicted for the trigonal structure obtained from the lithium compound, it is found to be negligible for the tetragonal $CuFeS_2$ phase obtained from $KCuFeS_2$. This different behavior is suggested to be responsible for the phase transition observed for the first case at moderate temperatures. This case is a nice illustration on how accurate modern quantum chemical calculations are able to provide valuable information on the relative stability of alternative structures for solid-state compounds even in complex cases where the origin of the instability in a given structure can be ascribed to fast atomic diffusion and not to thermodynamical factors.

AUTHOR INFORMATION

Corresponding Author

*E-mail: p.alemany@ub.edu.

ACKNOWLEDGMENTS

This work was supported by Proyectos de la Dirección de Investigación, U. de Antofagasta (Grant DI-CODEI-2010-01), FONDECYT (Grant 1090327 and 1110555), Fundación Andes (Grant 14055(2005)), DGI − Spanish Govenment (Project CTQ2008-06670-C02-02/BQU), and the Generalitat de Catalunya (Project 2009SGR-1459). S.C. gratefully acknowledges the Becas Chile program for a doctoral grant at the Universitat de Barcelona. The stay of P.A. at the U. Católica del Norte was made possible by FONDECYT (project 1090327).

REFERENCES

(1) Fong, R.; Dahn, J. R.; Batchelor, R. J.; Einstein, F. W. B.; Jones, C. H. W. *Phys. Rev. B.* **1989**, *39*, 4424−4429.
(2) Llanos, J.; Contreras-Ortega, C.; Mujica, C.; Von Schnering, H. G.; Peters, K. *Mater. Res. Bull.* **1993**, *28*, 39−44.
(3) Mujica, C.; Paez, J.; Llanos, J. *Mater. Res. Bull.* **1994**, *29*, 263−268.
(4) Llanos, J.; Valenzuela, P.; Mujica, C.; Buljan, A.; Ramirez, R. *J. Solid State Chem.* **1996**, *122*, 31−35.
(5) Llanos, J.; Buljan, A.; Mujica, C.; Ramirez, R. *J. Alloys Compd.* **1996**, *234*, 40−42.
(6) Llanos, J.; Buljan, A.; Mujica, C.; Ramirez, R. *Mater. Res. Bull.* **1995**, *30*, 43−48.
(7) Oledzka, M.; Ramanujachary, K. V.; Greenblatt, M. *Chem. Mater.* **1996**, *31*, 1491−1499.
(8) Oledzka, M.; Ramanujachary, K. V.; Greenblatt, M. *Chem. Mater.* **1998**, *10*, 322−328.
(9) Ramirez, R.; Buljan, A.; Noya, J. C.; Llanos, J. *J. Chem. Phys.* **1994**, *189*, 585−591.
(10) Llanos, J.; Buljan, A.; Mujica, C. *Bol. Soc. Chil. Quim.* **1995**, *40*, 227−231.
(11) Ramirez, R.; Mujica, C.; Buljan, A.; Llanos, J. *Bol. Soc. Chil. Quim.* **2001**, *46*, 235−245.
(12) Mujica, C.; Durán, R.; Llanos, J.; Clavijo, R. *Mater. Res. Bull.* **1996**, *31*, 483−486.
(13) Soler, J. M.; Artacho, E.; Gale, J. D.; Garcia, A.; Junquera, J.; Ordejón, P.; Sánchez-Portal, D. *J. Phys.: Condens. Matter.* **2002**, *14*, 2745−2779.
(14) For a review on applications of the SIESTA approach in materials science, see: Sánchez-Portal, D.; Ordejón, P.; Canadell, E. *Struct. Bonding (Berlin)* **2004**, *113*, 103−170.
(15) For more information on the SIESTA code visit: http://www.icmab.es/siesta
(16) Perdew, J. P.; Burker, K.; Ernzerhof, M. *Phys. Rev. Lett.* **1996**, *77*, 3865−3868.
(17) Troullier, N.; Martins, J. L. *Phys. Rev. B.* **1991**, *43*, 1993−2006.

(18) Kleinman, L.; Bylander, D. M. *Phys. Rev. Lett.* **1982**, *48*, 1425−1428.
(19) Artacho, E.; Sánchez-Portal, D.; Ordejón, P.; García, A.; Soler, J. M. *Phys. Stat. Sol. B* **1999**, *215*, 809−817.
(20) Monkhorst, H. J.; Park, J. D. *Phys. Rev. B.* **1976**, *13*, 5188−5192.
(21) Murnaghan, F. D. *Proc. Natl. Acad. Sci. USA.* **1944**, *30*, 244−247.
(22) Conejeros, C.; Sánchez, V.; Llanos, J.; Alemany, P.; Padilla-Campos, L. *Z. Kristallogr.* **2010**, *225*, 475−477.
(23) Shiang, K. D. *J. Chem. Phys.* **1993**, *99*, 9994−10000.
(24) Padilla-Campos, L.; Toro-Labbe, A. *J. Mol. Struct. (THEOCHEM).* **1997**, *390*, 183−192.
(25) Padilla-Campos, L.; Toro-Labbe, A. *J. Mol. Struct. (THEOCHEM)* **1995**, *330*, 223−229.
(26) Van der Ven, A.; Ceder, G. *Phys. Rev. Lett.* **2005**, *94*, 045901−1−045901−4.
(27) Jang, Y. I.; Neudecker, B. J.; Dudney, N. J. *Electrochem. Solid-State Lett.* **2001**, *4*, A74−A77.
(28) Aydinol, M. K.; Kohan, A. F.; Ceder, G.; Cho, K.; Joannopoulos, J. *Phys. Rev. B.* **1997**, *56*, 1354−1365.
(29) Le Bacq, O.; Pasturel, A.; Bengone, O. *Phys. Rev. B.* **2004**, *69*, 245107−1−245107−10.
(30) Zhou, F.; Cococcioni, M.; Kang, K.; Ceder, G. *Electrochem. Commun.* **2004**, *6*, 1144−1148.
(31) Zhou, F.; Cococcioni, M.; Marianetti, C. A.; Morgan, D.; Ceder, G. *Phys. Rev. B.* **2004**, *70*, 235121−1−235121−8.
(32) Zhou, F.; Marianetti, C. A.; Cococcioni, M.; Morgan, D.; Ceder, G. *Phys. Rev. B.* **2004**, *69*, 201101−1−201101−4.
(33) Arroyo de Dompablo, M. E.; Gallardo-Amores, J. M.; Amador, U. *Electrochem. Solid State Lett.* **2005**, *8*, A564−A569.
(34) Ceder, G.; Van der Ven, A.; Aydinol, M. K. *JOM—J. Min. Met. Mat. S* **1998**, *50*, 35−40.